Journal of Inflammation Research Dovepress

Open Access Full Text Article ORIGINAL RESEARCH

Decoding the Ferroptosis-Related Gene Signatures and Immune Infiltration Patterns in Ovarian Cancer: Bioinformatic Prediction Integrated with Experimental Validation

Beilei Zhang[1,*], Bin Guo[1,*], Hancun Kong[2,*], Linwei Yang[2], Hui Yan[2], Jierui Liu[2], Yichen Zhou[2], Ruifang An[1], Fu Wang[2–4]

[1]Department of Obstetrics and Gynecology, The First Affiliated Hospital of Xi'an Jiaotong University, Xi'an, Shaanxi, 710061, People's Republic of China; [2]Department of Medical Oncology, The Second Affiliated Hospital of Xi'an Jiaotong University, Xi'an, Shaanxi, 710004, People's Republic of China; [3]Department of Biophysics, School of Basic Medical Sciences, Xi'an Jiaotong University, Xi'an, Shaanxi, 710061, People's Republic of China; [4]School of Pharmacy, Shaanxi University of International Trade & Commerce, Xianyang, Shaanxi, 712046, People's Republic of China

*These authors contributed equally to this work

Correspondence: Ruifang An; Fu Wang, Email anruifang@163.com; wangfu@xjtu.edu.cn

Background: Ovarian cancer is a type of gynecological cancer with extremely high fatality rate. Ferroptosis, an iron-dependent regulated cell death, inhibits the immune infiltration of tumor cells. Therefore, it is worthwhile to explore the effects of ferroptosis-related gene signatures and immune infiltration patterns on the clinical prognosis of ovarian cancer.

Methods: In this study, we used the mRNA expression matrix and related medical information of those who suffer from ovarian cancer in the TCGA database. After that, we established a ferroptosis-related gene signature based on LASSO Cox regression model, and employed several specific enrichment analyses to explore the bioinformatics functions of differentially expressed genes (DEGs). Additionally, we analyzed the link between ferroptosis and immune cells by single-sample gene set enrichment analysis (ssGSEA) to create a heatmap of gene-immune cell correlation. We then examined the expression of immune checkpoints and verified the gene expression in ovarian cancer tissues by qPCR assays. Finally, we induced ferroptosis in ovarian cancer cells using drugs and analyzed their migration, invasion and gene expression.

Results: According to LASSO Cox regression analysis, 9 prognostic DEGs were in association with overall survival (OS), which was utilized to construct a 9-gene signature for patients. Patients were divided into two groups, in which high-risk group's OS was markedly shorter than that of low-risk group (Log−rank $p<0.001$). KEGG enrichment analysis showed that these DEGs were linked to human cytomegalovirus (HCMV) infection. The ssGSEA analysis revealed significant differences in immune cell type and expression between ALOX12 and GLRX5 groups ($p<0.05$). Heatmap showed high correlation of prognostic genes with various immune cells. qPCR assay confirmed the 9 gene expression signature in ovarian cancer tissues. The ovarian cancer cell invasion and migration were significantly inhibited after induction of ferroptosis.

Conclusion: We decoded the ferroptosis-related gene signatures and immune infiltration patterns that can be used to predict the prognosis of ovarian cancer patients.

Keywords: ovarian cancer, ferroptosis, tumor prognosis, gene signature, immune infiltration

Introduction

Ovarian cancer, a common type of gynecological cancer, has high fatality rate that ranks the first in the female reproductive system malignancies.[1] It is mainly derived from the germinal epithelial, germ cell, and sex cord-stromal, and may also be a malignant tumor transferred from the gastrointestinal tract.[2] Up to now, many subspecies of ovarian cancers have been found, among which high-grade serous ovarian cancer (HGSOC), ovarian clear cell carcinoma (OCCC), and mucinous

Received: 30 September 2024
Accepted: 27 November 2024
Published: 4 December 2024

carcinoma (MC) are more common.[3] In addition, great differences can be found in the forms of different subspecies of ovarian cancers. The occurrence of HGSOC, for example, is mostly due to the mutation of p53, though the proportion of p53 mutation in OCCC is very low.[4,5] The current treatment strategy for ovarian cancer is mainly based on its histological classification and staging, including cytoreductive surgery, chemotherapy as well as immunotherapy.[2] Generally speaking, a typical therapy includes staging surgery, tumor debulking surgery, and then platinum-based combination chemotherapy. Despite the continuous improvement of diagnosis and treatment, most of ovarian cancers still have the possibility of recurrence and eventually become drug-resistant cancer, so the 5-year OS of ovarian cancer patients has been less than 50%.[6,7] Prognostic models are often used to predict the risk of future events, such as the probability of cancer recurrence or postoperative death.[8] Considering the poor prognostic results of ovarian cancer patients and the limitations of existing prognostic models, a novel prognostic model with excellent effects on ovarian cancer is urgently needed.

Cell death is a universal phenomenon in nature, which is usually sorted into two categories: accidental cell death (ACD) and regulated cell death (RCD). Compared with the former, RCD is regulated by strict molecular mechanisms.[9] Ferroptosis is a kind of RCD featuring an excessive accumulation of phospholipid peroxidation regulated by numerous cellular metabolic activities.[10] It should be noted that drug-resistant cancers, especially mesenchymal and metastatic cancer cells, can be easily affected by ferroptosis. Consequently, much attention has been paid to the immense value of ferroptosis in treating diseases like drug-resistant cancers. In recent years, substantial studies have found regulatory genes or ferroptosis markers. Glutathione peroxidase 4 (GPX4), expressed by GPX4 gene, could change lipid hydroperoxides into non-toxic lipid alcohols to inhibit ferroptosis.[11–13] At present, many studies have associated ferroptosis with ovarian cancer, but the bond between partial genes and the prognosis of ovarian cancer is not so clear.

Besides cancer cells, ovarian cancer is also composed of epithelial cells, fibroblasts, and immune infiltrating cells, which constitute the tumor microenvironment.[14–16] Among them, tumor immune infiltrating cells are essential to the growth and diffusion of tumor cells. It consists of white blood cells, red blood cells, and other cell groups. Recent researches have verified that several victims of ovarian cancer display an anti-tumor immune response spontaneously characterized by tumor-reactive T cells and/or antibodies. In addition, the more lymphocytic infiltration can be seen in tumors, the better OS ovarian cancer patients have.[17–19] However, the rise in the ratio of T regulatory cells, which mediate immunosuppression, usually predicts worse OS in patients.[20] Other immunosuppressive cell subtypes, such as tumor macrophages expressing B7-H4, are also associated with adverse outcomes.[21] Tumor immune infiltrating cells have become a new target for tumor therapy and provide opportunities for the improvement of new treatment options. Nowadays, there is a popular view that infiltrating immune cells should be taken into consideration while predicting the prognosis of cancer patients.[22] Consequently, it's vital to integrate immune infiltration patterns into the model.

Material and Methods

Data Acquisition

We collected 354 ovarian cancer patients' information from Genomic Data Commons The Cancer Genome Atlas (GDC TCGA) on the UCSC Xena (https://xenabrowser.net/datapages/) platform for survival analysis and immune assessment. In GDC TCGA, the data on normal ovary samples were missed, so we used the TCGA and GTEx (Genotype-Tissue Expression) joint database to perform difference analysis on the counts data of 420 ovarian cancer and 88 normal ovarian samples to screen DEGs. The TCGA and GTEx databases used in the experiment are public, so there is no need for the permission of the ethics committee. Nevertheless, our study strictly obeys the data access policy and publication guidelines of TCGA and GTEx. The data on ferroptosis-related genes (FRGs) were from the FerrDb database (http://www.zhounan.org/ferrdb/current/).[23] Among them, driver, suppressor and marker genes were obtained for screening DEGs related to ferroptosis.

Construction and Verification of Prognostic Characteristics of Genes Associated with Ferroptosis

All the FRGs were filtered by the "DESeq2" R package (|Log2FoldChange| > 1, p.adjust < 0.05), and 180 DEGs related to ferroptosis were obtained. The Benjamini & Hochberg (BH) method was used to correct the p-value (Driver: 95; Suppressor: 92; Marker: 6, Supplementary Table S1). We established a protein-protein interaction network (PPI) using

the STRING database (version 11.5, https://string-db.org/). Then, univariate Cox regression analysis was conducted to find the genes associated with prognosis. ($p<0.05$). On this basis, LASSO-penalized Cox regression analysis, which can reduce overfitting risk, was applied to construct a prognostic model. We utilized the "glmnet" R package to select and shrink the variables of the LASSO algorithm. In this regression analysis, gene normalized expression matrix was the independent variable, while patients' OS and survival status were dependent variables. The penalty coefficient λ is determined based on the minimum standard ten-fold cross-validation. We calculated the patient risk scores derived from each gene's normalized expression levels and their corresponding regression coefficients. High risk group, as well as low risk group, were set in accordance with the medium score. The time-dependent ROC curve was performed to test the risk score's predictive effect on survival time using the "timeROC" R package.

Functional Enrichment Analysis

We utilized the "clusterProfiler" R package to enrich the 180 DEGs by Gene Ontology (GO) and Kyoto Encyclopedia of Genes and Genomes (KEGG) pathways (| Log2FoldChange | > 1, p.adjust < 0.05). The BH method was used to correct the p-value.

Immune and Gene Level Analysis

To investigate the association between 22 kinds of immune cells and 9 prognostic genes, we used the correlation analysis between gene expression in the "corrplot" R package and ciber to draw a correlation heatmap. We extracted and consistently clustered the expression of ALOX12 and GLRX5 by using the "ConsensusClusterPlus" R package, which can divide the ovarian cancer tissue samples into two clusters. The immune cell infiltration scores of 28 species were evaluated by mapping the ssGSEA score comparison boxplot from both groups using ssGSEA in the "gsva" R package. Finally, we used the "ggplot2" R package to analyze the differential expression of 13 common immune checkpoints, drew the box plot of immune correlation analysis, and discussed the correlation between immune checkpoints and prognostic genes.

Ovarian Cancer Samples Collection and qPCR Assay

All operations have been approved by the Biomedical Ethics Committee of Xi'an Jiao Tong University and complies with the Declaration of Helsinki. And the informed consent was obtained from patients. Each twenty tissue samples were collected from both ovarian cancer patients and normal peoples at the First Affiliated Hospital of Xi'an Jiao Tong University. To detect the nine gene expression in tissue samples, the RNA Extraction Kit (Qiagen) was used to isolate total RNA from tissue samples in each group following the manufacturer's instructions. RNA concentration was determined using the NanoDrop (ThermoFisher Scientific). Subsequently, the RNA was reverse-transcribed to cDNA using the QIAGEN OneStep RT-PCR Kit. The SYBR Green qPCR Kit was used to perform the qPCR assay with the Real-Time PCR System (Applied Biosystems, USA). The qPCR conditions were set as follows: 95°C for 30s, 40 cycles of 95°C for 10s, and 58°C for 30s. The relative expression levels of genes were normalized to GAPDH and calculated using the $2^{-\Delta\Delta CT}$ method.

Cell Culture Assay

Skov3 cells (human ovarian adenocarcinoma cells) were purchased from ATCC cell bank and cultured in high-glucose DMEM medium (Hyclone) supple mented with 10% fetal bovine serum (FBS, Gibco) and 1% penicillin-streptomycin solution (Hyclone). All the cells were grown at 37°C under 5% CO_2 humidity. Skov3 cells were seeded in 12-well plates and incubate overnight to achieve approximately 100% cell coverage. A line within the cell layer was scraped by a p10 pipette tip, and then each well was rinse twice with PBS to clear cellular debris. The cells were then incubated in DMEM medium containing 1% FBS and RSL3 (200 nmol/mL). The wound closure was observed by microscopy at 0 and 12 hours and the relative recover area of wound healing was calculated with ImageJ software. A Transwell chamber (8 m pore size; Corning, USA) coated with Matrigel matrix was used to measure cell invasion. First, 200 nM RSL3-treated cells were collected with untreated cells, and 1×100 cells/mL cell suspension was prepared by resuspending the cells with serum-free DMEM. Subsequently, 200 μL cell suspension and 600 μL DMEM medium supplemented with

10% FBS were added to the upper and lower chamber respectively. After incubation for 36 h in a 5% CO2 cell incubator at 37 °C, we fixed the invaded cells with methanol and then stained them using 1% crystal violet. At last, the invaded cells were counted with a microscope.

MTT Assay

The Skov3 cells were seeded in 96-well plates (1×10^4 cells/well). The next day, the medium was replaced with medium containing different concentrations of the RSL3. After incubation for 12 hours, the cells were further treated with 100mL of medium containing 0.5 mg/mL MTT for 4 hours. After that, the supernatant was removed from the well, then the formamide formed by living cells was dissolved by 100 uL DMSO, and the absorbance at 490 nm was measured using a microplate reader (SuPerMax 3100, Flash, China).

Statistical Analysis

P value was used to judge statistical significance. $P < 0.05$ was considered as a significant difference. Every statistical analysis was carried out using the following packages in R software (version 4.2.1): DESeq2, forestplot, survival, glmnet, caret, timeROC, tidyverse, coin, clusterProfiler, org.Hs.eg.db, ggplot2, GOplot, stringr, gsva, corrplot, and ConsensusClusterPlus.

Results

Filtration of Prognostic Genes and Construction of Interaction Network

The flowchart of our study is illustrated in Supplementary Figure S1. After disposal, a total of 180 FRGs were found to differ in terms of gene expression profiles between tumor and normal tissues. Therefore, we performed univariate Cox regression analysis and obtained 12 genes related to OS ($p < 0.05$, Figure 1A). The heatmap showed the expression differences of 12 genes between tumor and normal ovarian tissues (Figure 1B). In addition, the PPI network (threshold of the lowest interaction score: 0.150) presented the interaction among these 12 genes (Figure 1C).

Construction of a Prognostic Model of Ovarian Cancer Using 9 Ferroptosis-Related Genes

Because the TCGA.04.1357.01A sample data in the TCGA database is partially missing, the sample is excluded in subsequent analysis. The prognostic model of ovarian cancer patients was screened and established from 12 genes obtained by LASSO Cox regression analysis. Using the optimal value of the penalty parameter λ (Figure 2A and B), we obtained 9 independent prognostic genes, which constituted a 9-gene signature, and used it to establish a multivariate Cox regression analysis model (Supplementary Figure S2). The risk score was derived for an individual patient by the following formula: risk score = (−0.27726)*GLRX5 + 0.36772*ALOX12 + (−0.31664)*KLHDC3 + (−0.34698) *SLC7A11 + (−0.07417)*SOX2 + (−0.18872)*FH + (−0.20477)*GCH1 + (−0.07378)*MYCN + (−0.13949)*FURIN. According to the risk score of each patient, we divided the patients into a high-risk group (n=176) and a low-risk group (n=177) by the median risk score of all patients (Figure 2C, the median risk score was 0.996788). Kaplan-Meier survival curves showed that patients in the high-risk group had worse OS compared to those in the low-risk group (Log-rank $p < 0.001$, Figure 2D). The predictive effect of the risk score for OS was reflected by the time-dependent ROC curve. The area under the curve (AUC) was 0.699 for 1 year, 0.666 for 3 years, and 0.727 for 5 years (Figure 2E).

Independent Prognostic Value of the 9-Gene Signature

We used univariate and multivariate Cox regression analysis for clinical variables to test if the risk score had a significant prognostic value for OS. Subsequently, it was found that the risk score could be used as an independent predictor of OS. In univariate Cox regression analysis, HR = 2.00045, 95% CI = 1.691–2.367, $p < 0.001$ (Figure 3A); in multivariate Cox regression analysis, although other factors were corrected, the data results indicate that the risk score could still independently predict the OS, HR = 1.937, 95% CI = 1.633–2.297, $p < 0.001$ (Figure 3B).

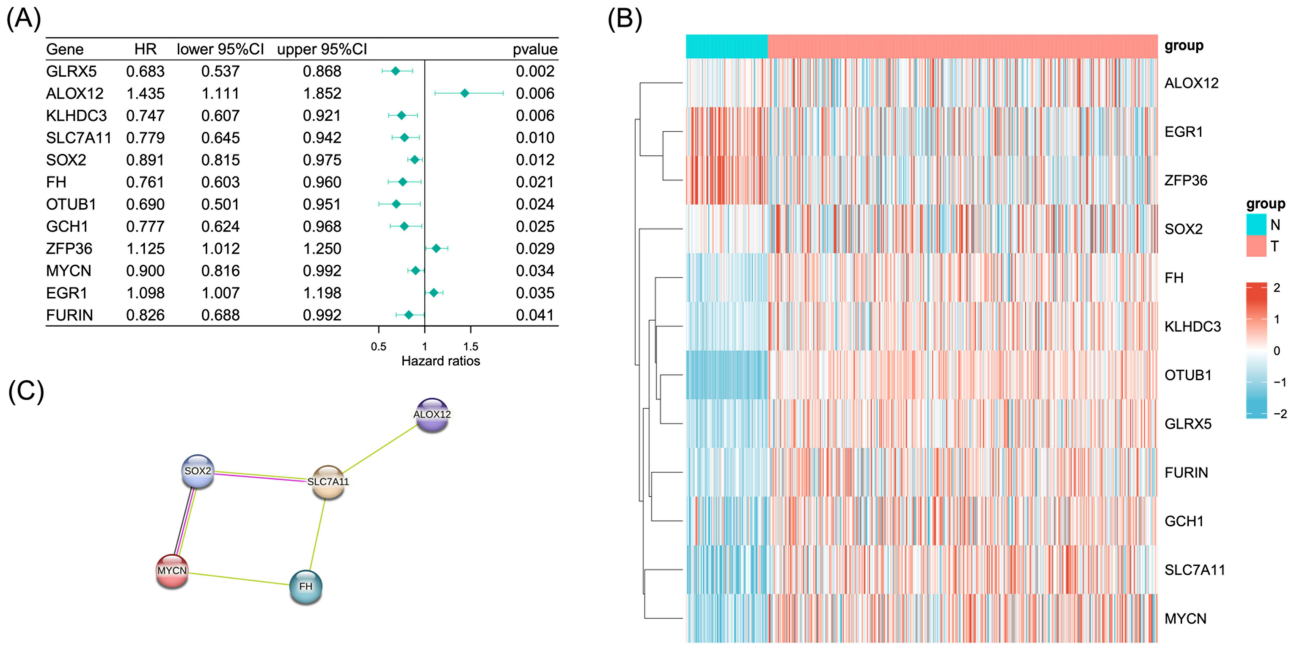

Figure 1 (**A**) The forest plot of univariate regression analysis showed a strong relationship between 12 prognostic FRGs and OS. (**B**) The expression differences of these 12 prognostic genes in tumor and normal tissues. (**C**) The PPI network in the STRING database shows the interaction between these 12 prognostic genes.

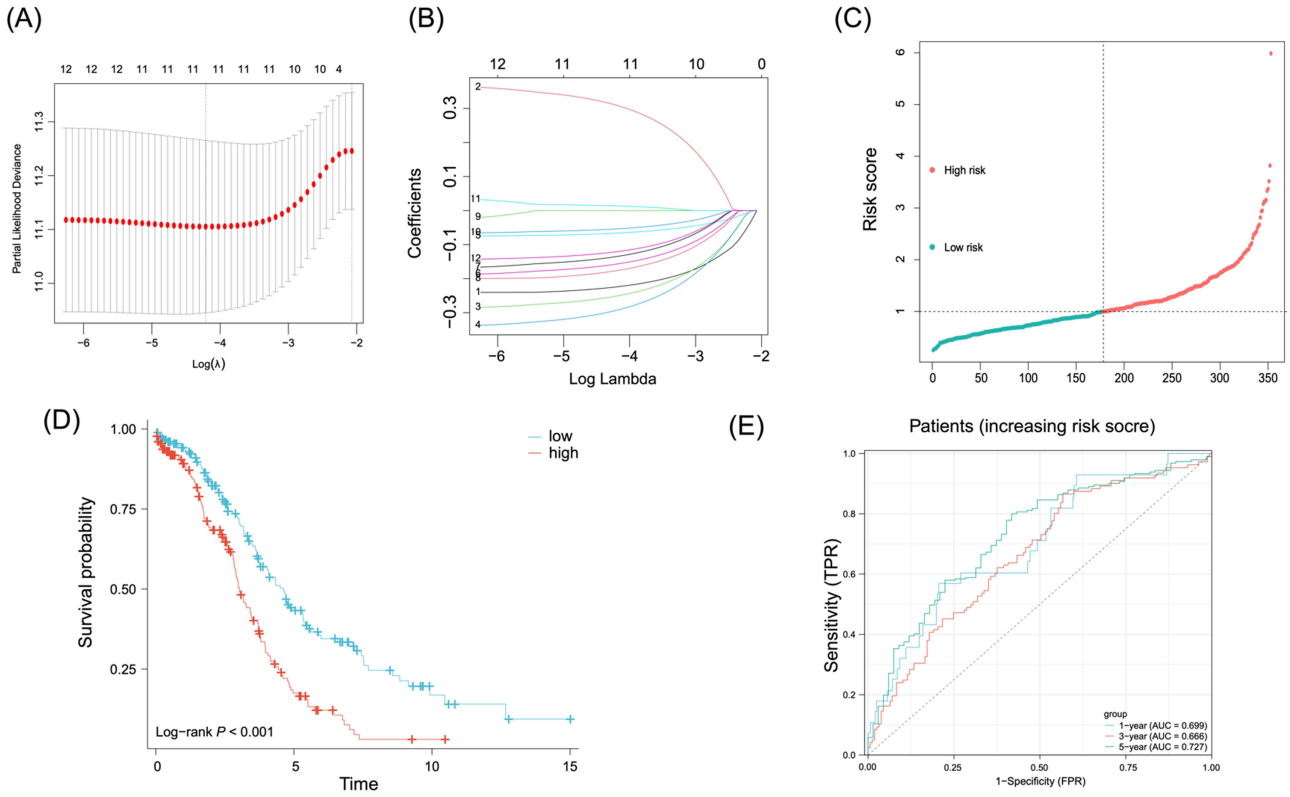

Figure 2 (**A** and **B**) Ferroptosis-related gene signature model diagnosis process LASSO Cox regression analysis curve. (**C**) Model-based risk scores were used to classify patients into high and low risk groups. (**D**) Kaplan-Meier curve of overall survival in high and low risk groups. (**E**) The time-dependent ROC curve.

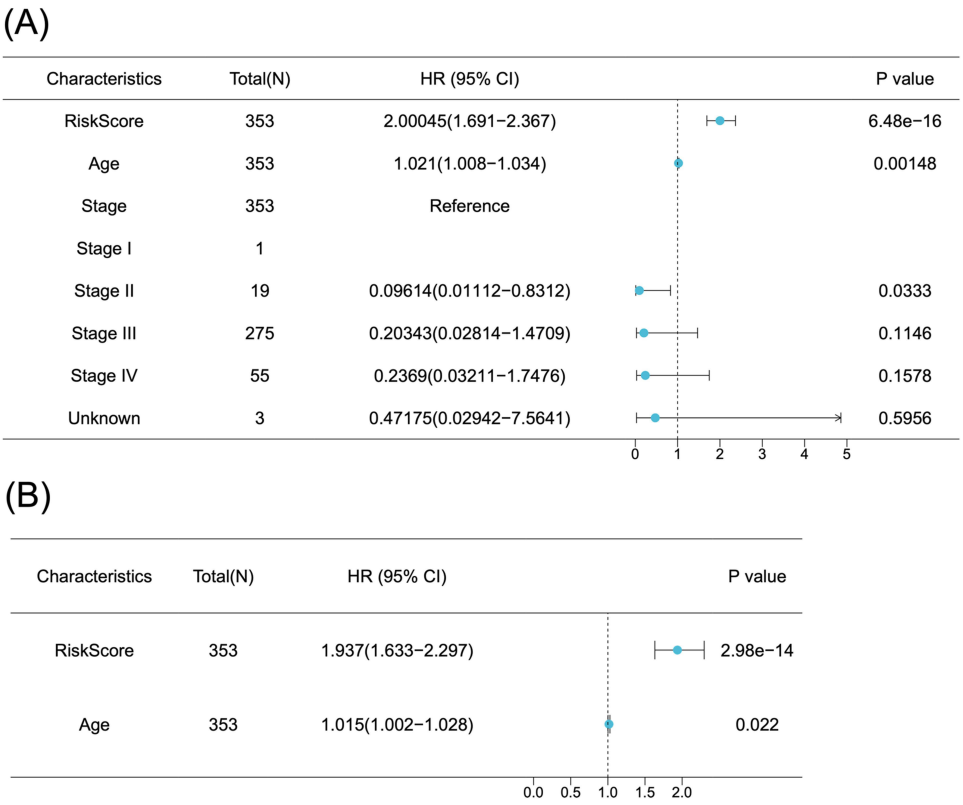

Figure 3 The relationship between clinicopathological factors and OS in (**A**) univariate and (**B**) multivariate Cox regression analysis.

Functional Enrichment Analysis

We resorted to GO and KEGG functional analysis to elucidate the biological functions and pathways of ferroptosis-related DEGs. In GO enrichment analysis, DEGs enriched fatty acid metabolism processes and multiple oxidative stress and iron-related pathways, such as cell response to oxidative stress, iron ion metabolism homeostasis, and other processes ($P < 0.05$, Figure 4A and B). In KEGG pathway analysis, prognostic genes were enriched in ferroptosis and multiple important biological metabolic pathways, such as the glutathione metabolism, p53 signaling pathway, and mTOR signaling pathway ($P < 0.05$, Figure 4C and D). Moreover, we found that the network composed of ALOX12, SLC7A11, and FH made a great deal of difference in regulating ferroptosis in ovarian cancer in the PPI network constructed in the STRING database.[24] In addition, DEGs play an important part in HCMV infection and significantly impact the immune microenvironment, indicating a certain relationship with tumor immune infiltration.

Immune Cell Enrichment Analysis

We explored the characteristics of immune cells and their relationship with FRGs. By analyzing the correspondence between the expression of FRGs and ciber, we obtained the correlation heat map between 22 immune cells and 9 prognostic genes (GLRX5, ALOX12, KLHDC3, SLC7A11, SOX2, FH, GCH1, MYCN, and FURIN). The results showed that multiple prognostic genes had a high correlation with different immune cells, and the detailed information was shown in Figure 5.

For further searching to examine the connection between immune cells and risk scores, we quantified the enrichment scores of 28 immune cell subsets with the ssGSEA method. The results showed significant differences between the two sets of data on immune cell types obtained by clustering the prognostic genes ALOX12 and GLRX5 (Figure 6).

The analysis of immune correlation showed prominent differences in the expression levels of immune checkpoints (PDCD1, CD274, PDCD1LG2, LAG3, EGR1, CD160, NRP1, LGALS9, and LILRB2) between the two groups of data gained from the previous clustering (Figure 7).

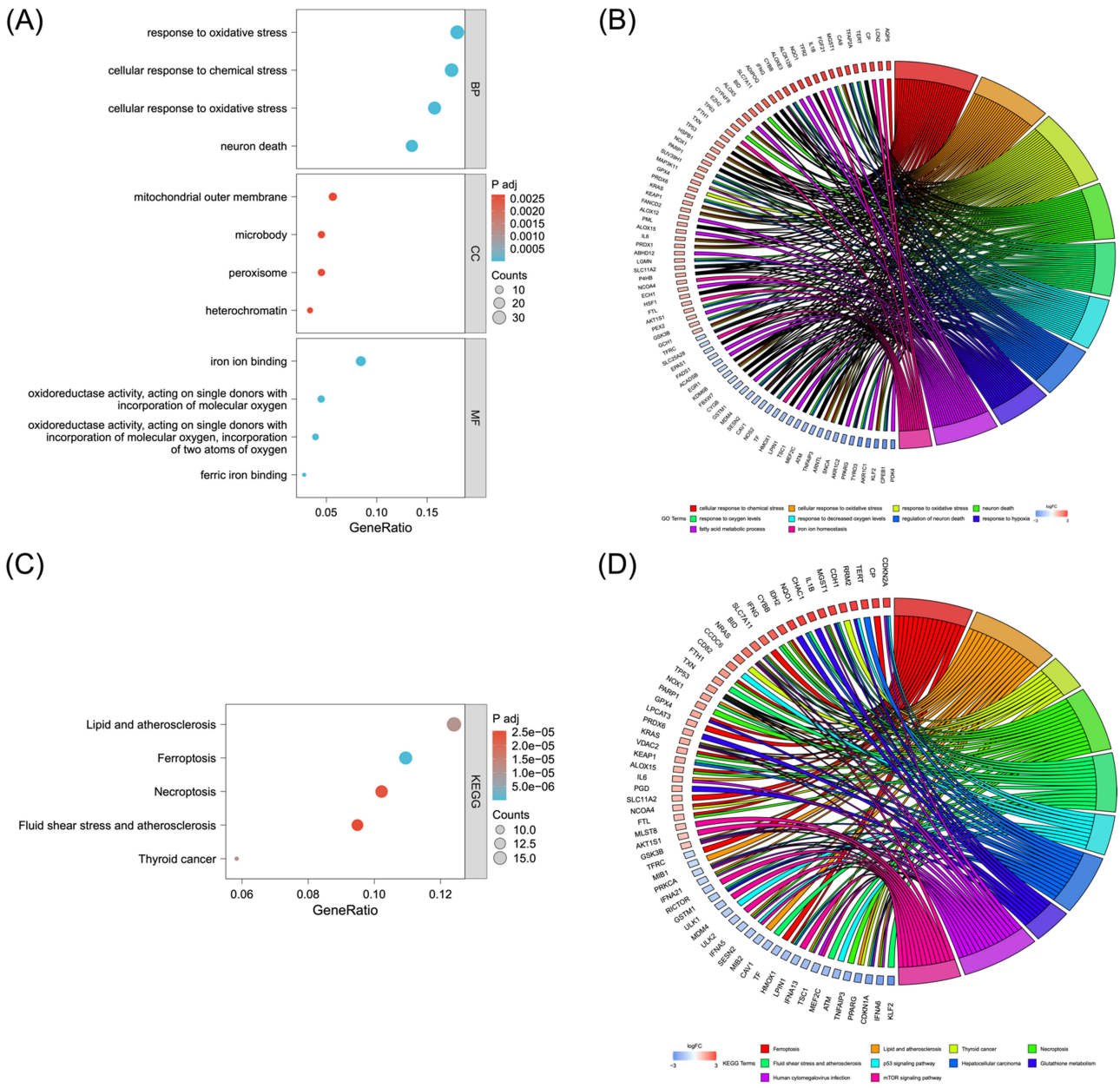

Figure 4 The representative results of ferroptosis-related DEGs in GO (**A** and **B**) and KEGG (**C** and **D**) enrichment analysis.

Validation of the Expression of 9 Prognostic Genes in Ovarian Cancer Samples

To validate the expression of the 9 prognostic genes (GLRX5, ALOX12, KLHDC3, SLC7A11, SOX2, FH, GCH1, MYCN, and FURIN) in ovarian cancer, each 20 tissue samples from both ovarian cancer patients and normal peoples were collected and the expression of these genes were detected by qPCR assay. As shown in Figure 8A–I, compared to that in the normal ovarian tissue samples, the expression levels of 8 genes (GLRX5, KLHDC3, SLC7A11, SOX2, FH, GCH1, MYCN, and FURIN) in ovarian cancer tissues were significantly upregulated, whereas ALOX12 expression was downregulated, which was consistent with our bioinformatic analysis.

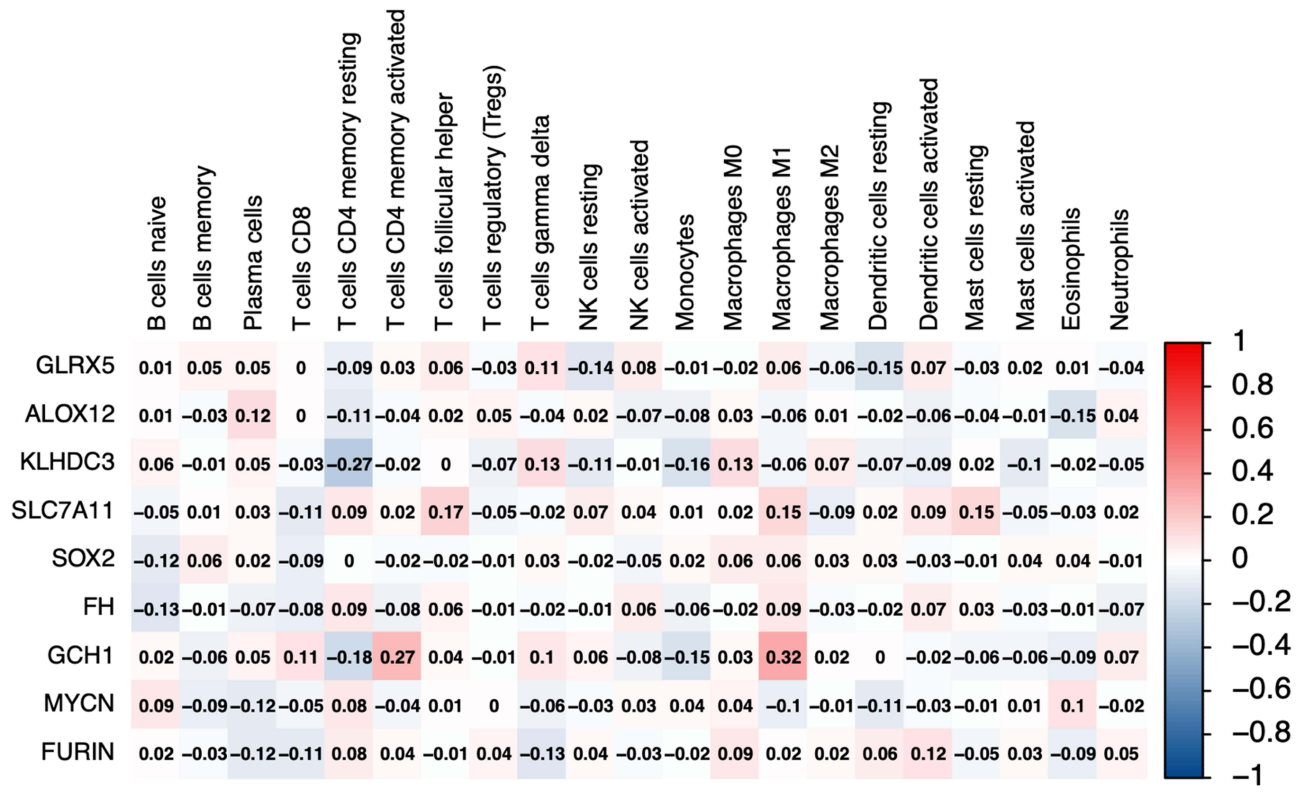

Figure 5 Correlation heat map of gene expression and ciber. Red represents up, blue represents down.

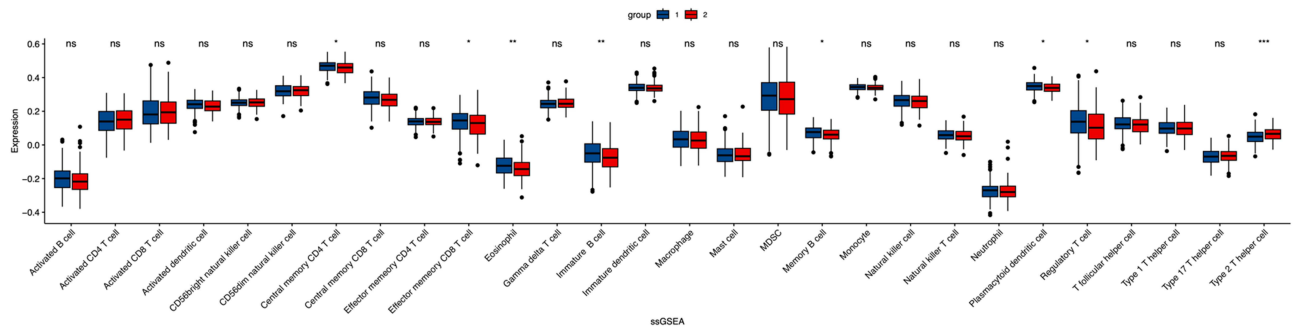

Figure 6 Comparison of ssGSEA scores between group 1 and group 2, obtained by clustering the prognostic genes ALOX12 and GLRX5. (Group 1: relatively higher expression of GLRX5 and lower expression of ALOX12. Group 2: relatively higher expression of ALOX12 and lower expression of GLRX5.) The box plot shows the scores of 28 immune cells. The adjusted p-value is shown as: ns, not significant; * p<0.05; ** p<0.01; *** p<0.001.

Gene Expression and Cell Survival in RSL3-Induced Ferroptosis in Ovarian Cancer Cells

RSL3 is a VDAC-independent ferroptosis activator and an inhibitor of GPX4, which binds and inactivates GPX4 and then mediates GPX4-regulated ferroptosis.[25,26] To further explore the gene expression of ferroptosis in ovarian cancer cells, we induced ferroptosis in Skov3 cells using RSL3. Different concentrations of RSL3 were added to Skov3 cells and then subjected to MTT assay. The results showed that the cell viability decreased continuously with the increase of RSL3 concentration (Figure 9A). In addition, we also detected the mRNA expression levels of ALOX12 and GLRX5 by qRT-PCR. After RSL3 treatment, the mRNA expression level of ALOX12 increased significantly (Figure 9B), while there was a certain degree of decrease in the mRNA expression level of GLRX5 (Figure 9C). In addition, we also performed transwell invasion assay (Figure 9D and E) and wound healing assay (Figure 9F and G). It was shown that RSL3-induced ferroptosis significantly inhibited ovarian cancer cell viability and migration.

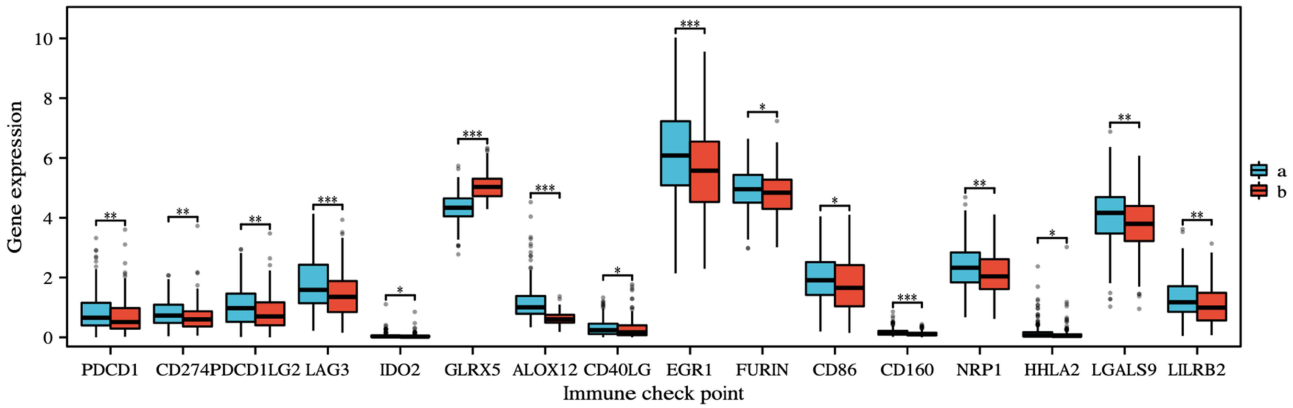

Figure 7 Immune correlation analysis box plot. The adjusted p-value is shown as: ns, not significant; * p<0.05; ** p<0.01; *** p<0.001.

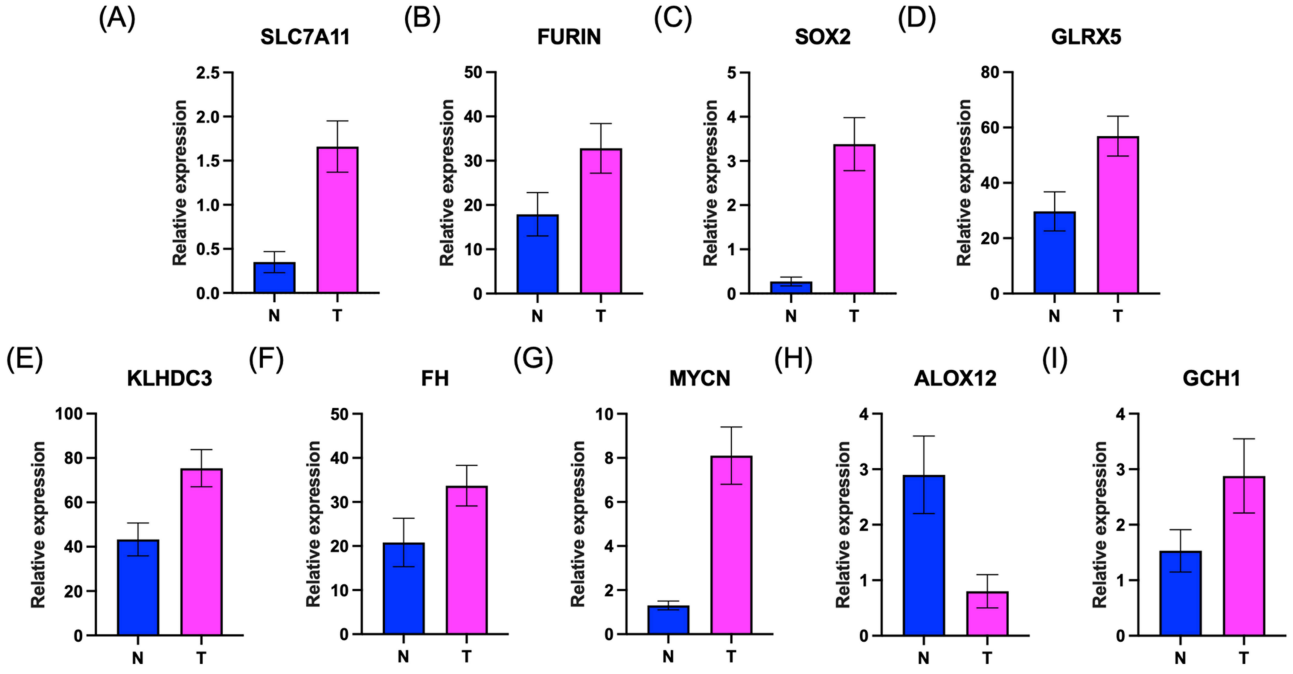

Figure 8 qPCR assay was performed to detect the expression of 9 genes (**A**) SLC7A11, (**B**) FURIN, (**C**) SOX2, (**D**) GLRX5, (**E**) KLHDC3, (**F**) FH, (**G**) MYCN, (**H**) ALOX12, and (**I**) GCH1 in tissue samples from ovarian cancer patients and normal people. (**N**) normal; (**T**) tumor.

Discussion

Due to the lack of screening tests, ovarian cancer is hard to be discovered in the early stage and is prone to recurrence after surgery. At present, surgical intervention represents a fundamental aspect of the treatment plan. A range of techniques have been investigated and refined with the objective of predicting the potential for achieving a residual tumor of 0 (RT=0).[27] Although many advances have been made in current treatment technology, such as the combination of BRAF inhibitor and MEK inhibitors for ovarian cancer,[28] it remains the most lethal cancer in female gynaecology. Ferroptosis is a new type of RCD, which is the result of oxidative damage and subsequent cell membrane damage caused by the accumulation of iron-dependent lipid hydroperoxide to a certain level.[29] Existing researches demonstrate that ferroptosis is strongly related to the occurrence and development of ovarian cancer, which can bring new hope to patients with ovarian cancer.[30]

In this study, we found that 180 DEGs in ovarian cancer tissues had 2-fold or more changes in expression levels compared with normal ovarian tissues, and established a new prognostic model using 9 independent prognostic genes.

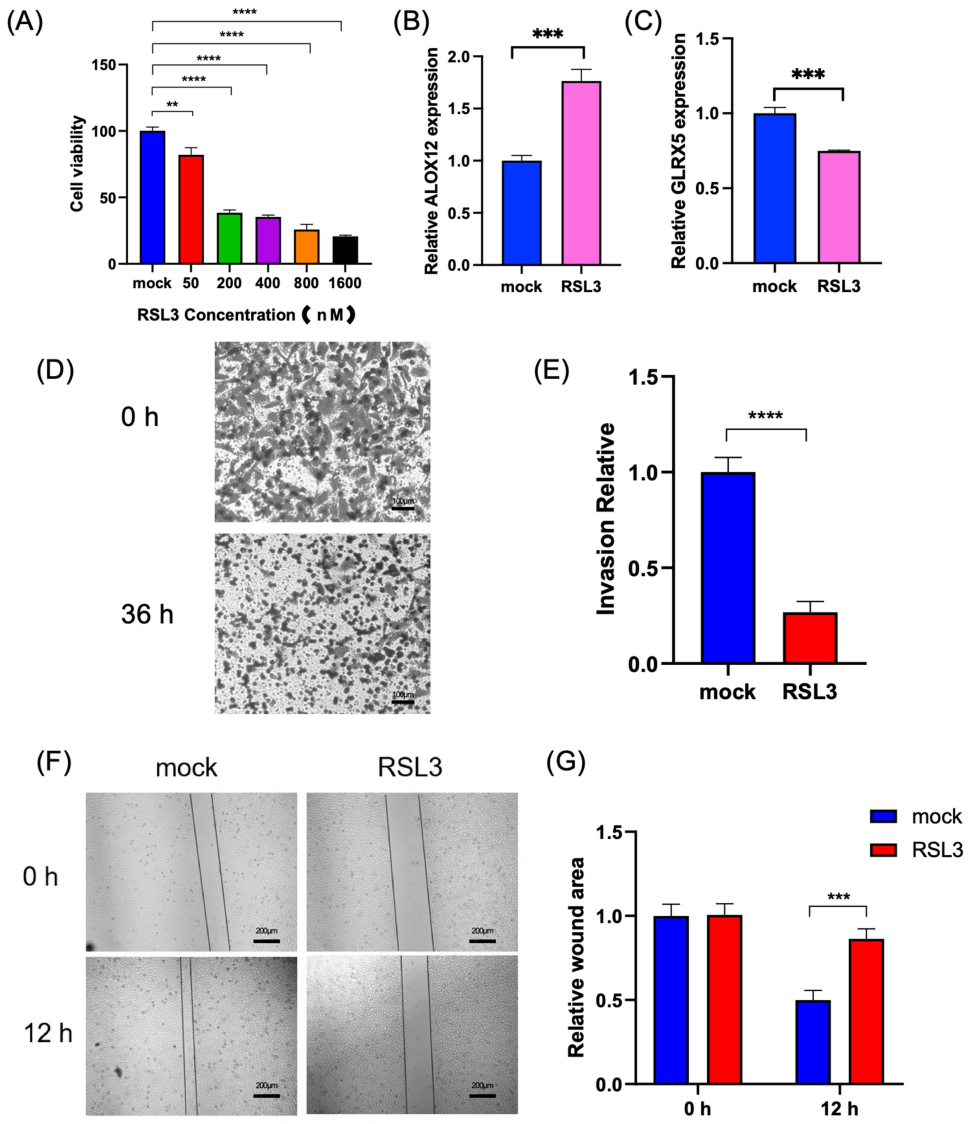

Figure 9 Effects of RSL3 in ovarian cancer cells. (**A**) Different concentrations of RSL3 were added to Skov3 cells and then cell viability was detected by MTT assay. (**B** and **C**) RT-qPCR assay of ALOX12, GLRX5 expression after induction using RSL3. Shows fold change in expression relative to control. (**D**) RSL3 was added to Skov3 cells and cell invasion was observed microscopically. (**E**) Transwell results were calculated by ImageJ software. (**F**) Cell healing of each group was imaged using a microscope at 0 h and 12 h. (**G**) The healed area was calculated by ImageJ software at different time points. The adjusted p-value is shown as: ** p<0.01; *** p<0.001; **** p<0.001.

Among them, the up-regulated expression of multiple risk genes led by ALOX12, and the down-regulated expression of multiple protective genes led by SLC7A11 promotes the process of tumor ferroptosis. Inhibition of GLRX5 causes tumor cells of cisplatin-resistant head and neck to enter the ferroptosis process of ferroptosis.[31] ALOX12 is on the short arm of chromosome 17 of 13.1, which is abnormally expressed in a variety of tumors. It has a variety of mechanisms including participating in amino acid metabolism to induce inflammation and promote lipid synthesis. And it is a potential marker of many cancers.[32] As a protective gene, its deletion is sufficient to accelerate tumor growth. In the generally accepted mechanism of ferroptosis, ACSL4 is indispensable, but the ALOX12 can be independent of ACSL4 and mediate p53-dependent tumor inhibition of ferroptosis.[33] KLHDC3 inhibits ferroptosis in vitro by removing the $p14^{ARF}$-mediated SLC7A11 transcriptional inhibition process to support tumor growth in vivo.[34] SLC7A11 is located in the q28-q32 position of the human chromosome 4's long arm, with a length of 78 kbp, containing 31 introns and 32 exons. SLC7A11 can promote the biosynthesis of glutathione (GSH) by introducing cysteine, thereby promoting GPX4-mediated lipid peroxide decomposition to inhibit the process of ferroptosis.[29] Cancer cells inhibit ferroptosis by overexpressing SLC7A11, thereby promoting tumor growth, but at the same time, cancer cells are also responsible for the large

consumption of glucose and glutamine in the SLC7A11-mediated metabolic process, this metabolic weakness provides new ideas for targeted therapy of cancer.[35]

The immunocyte enrichment analysis we performed reveals that ferroptosis has a close relationship with tumor immunity, and the view that immunity promotes or inhibits tumors has been widely accepted. Therefore, we found that ovarian cancer patients' immune status between the two groups of data obtained by clustering the prognostic genes ALOX12 and GLRX5 is significantly different, including the degree of tumor immune infiltration of central memory $CD4^+$ T cell, effector memory $CD8^+$ T cell, eosinophil, immature B cell, memory B cell, plasmacytoid dendritic cell, regulatory T cell, and Th2 cell. In addition, we found that DEGs were related to HCMV infection through KEGG enrichment analysis.

There are eight types of human herpesviruses and HCMV is one of them. It can hide in a host lifelong time and may become active again.[36] HCMV infection can induce T cell responses of some selected immunodominant epitopes. This immune response is named memory inflation, which is one of the most prominent features of HCMV infection. And the number of antigen-specific $CD8^+$ T cells showing the effect is slightly increased or maintained for a long time.[37–39] When the virus invades the human body and the immune is initiated, $CD8^+$ T cells usually respond by active proliferation of effector cells driven by antigens. Researchers have shown that the introduction of heterologous antigen epitopes into recombinant HCMV vectors can efficiently control viral infection. The more the number of viral genomes in the latent period, the more the latent transcripts increase, which leads to more antigen expression with stronger CD8 activation.[36] It is reported by recent studies have reported that HCMV protein and DNA exist in ovarian cancer tissues. HCMV acts as an inducer or promoter to promote carcinogenesis.[40–42] By encoding viral proteins and inducing various immunosuppressive cytokines, HCMV allows tumors to escape immune surveillance, which is conducive to tumor growth and leads to HCMV-induced immune tolerance.[43] HCMV will increase its adaptability in the weak immune environment of cancer cells, so HCMV superinfection can accelerate the development of cancer.[44] Researchers have observed that some HCMV strains have direct carcinogenic effects on cell stress, polyploid tumor giant cells, stem cells, and epithelial-mesenchymal transition, which can explain the appearance of invasive cancer during the treatment of adenocarcinoma with poor prognosis, metastasis, and drug resistance.[45]

A significant correlation exists between the prognosis gene GCH1 and $CD8^+$ T cells, showing how ferroptosis and immunity are intricately linked. The mysterious and complex relationship between immunity and ferroptosis is gradually being revealed[46] with the development of in vivo and in vitro experiments. Researchers found that $CD8^+$ T cells of tumor host can promote ferroptosis-specific lipid peroxidation and intensify ferroptosis by releasing interferon II, thus improving the immunotherapy's efficacy.[46] We found that there was a remarkable difference in $CD8^+$ T cell content between the two groups of data obtained by previous clustering. We think the reason is that $CD8^+$ T cells release signals (such as type II interferon) to activate ferroptosis.[46] But it is still needed to confirm the above results by more work.

Since the DEGs are related to HCMV infection, the correlation heatmap indicates that the prognostic gene GCH1 is in connection with the role of $CD8^+$ T cells, and HCMV infection will be inhibited by $CD8^+$ T cells, the prognosis of ovarian cancer patients infected with HCMV can be predicted by the expression of the prognosis gene GCH1, thus putting forward a new scheme to diagnosis and cure ovarian cancer patients who are infected with HCMV.

On the basis of our work, we compared the gene expression of 13 immune checkpoints of the two groups of data after clustering ALOX12 and GLOX5. Among them, the p values of three immune checkpoints (such as LAG3, EGR1, etc.) were less than 0.001, indicating that the cases obtained by clustering the two prognostic genes had very obvious differences in the expression of some immune checkpoints. Furthermore, the expression of both ALOX12 and GLOX5 genes differed after induction of iron death using the GPX4 inhibitor RSL3, which further proved that there was a certain relationship between ferroptosis-related prognostic genes and immune checkpoints, and played an important role in tumor immunotherapy.

In recent years, with the rise of immune checkpoint blockade therapy, immune checkpoint inhibitors (ICIs) have significantly changed how tumors are treated.[47] Lymphocyte-associated gene 3 (LAG3) is one of the immunoglobulin superfamilies, which is negative in the regulatory process of T cell activation and proliferation. It can be combined with major histocompatibility complex class II (MHC-II), which is conducive to tumor immune escape.[48] The antibody 8F-6 has great affinity with LAG3, which can block the combination of MHC-II and LAG3 so that T cells can return to the normal level, enhance immunity, and kill tumor cells. Early growth response 1 (EGR1) is a transcription factor containing

a zinc finger domain that can specifically recognize and bind to target genes and regulates their transcription.[49] Researches have shown that EGR1 is absent in a variety of malignant tumors. Nevertheless, in ovarian cancer tissue samples, EGR1 can promote the progress of ovarian cancer.[50] However, it is necessary to point out that the research on EGR1 immune blockers is still unclear and needs further in-depth exploration.

In conclusion, we utilized ferroptosis-related 9-gene signatures and immune infiltration patterns to construct a new prognostic model. Compared with previous prognostic models, this model has more significant prognostic ability, provides more accurate risk prediction and survival analysis, and can predict the survival time of patients more comprehensively, which would positively benefit the clinical application.

Data Sharing Statement

All the data are included in the manuscript and supplementary materials.

Ethics Statement

This study has been approved by the Biomedical Ethics Committee of Xi'an Jiaotong University and complies with the Declaration of Helsinki.

Funding

This work was supported by National Natural Science Foundation of China (No. 32271512), Natural Science Basic Research Program of Shaanxi (Program No. 2022JC-56, 2023-JC-ZD-43, 2023-JC-YB-660), the Foreign Expert Project of Ministry of Science and Technology of China (G2023174001L).

Disclosure

All authors declare no conflicts of interest.

References

1. Siegel RL, Miller KD, Fuchs HE, Jemal A. Cancer Statistics, 2021. *Cancer J Clin*. 2021;71:7–33. doi:10.3322/caac.21654
2. Jayson GC, Kohn EC, Kitchener HC, Ledermann JA. Ovarian cancer. *Lancet*. 2014;384:1376–1388. doi:10.1016/s0140-6736(13)62146-7
3. Seidman JD, Horkayne-Szakaly I, Haiba M, et al. The histologic type and stage distribution of ovarian carcinomas of surface epithelial origin. *Int J gyn pat*. 2004;23:41–44. doi:10.1097/01.pgp.0000101080.35393.16
4. Ahmed AA, Etemadmoghadam D, Temple J, et al. Driver mutations in TP53 are ubiquitous in high grade serous carcinoma of the ovary. *J path*. 2010;221:49–56. doi:10.1002/path.2696
5. Bolton KL, Chen D, Corona de la Fuente R, et al. Molecular Subclasses of Clear Cell Ovarian Carcinoma and Their Impact on Disease Behavior and Outcomes. *Clin can rese*. 2022;28:4947–4956. doi:10.1158/1078-0432.CCR-21-3817
6. Salani R, Khanna N, Frimer M, Bristow RE, Chen LM. An update on post-treatment surveillance and diagnosis of recurrence in women with gynecologic malignancies: society of Gynecologic Oncology (SGO) recommendations. *Gynecol Oncol*. 2017;146:3–10. doi:10.1016/j.ygyno.2017.03.022
7. Vaughan S, Coward JI, Bast RC, et al. Rethinking ovarian cancer: recommendations for improving outcomes. *Nat Rev Cancer*. 2011;11:719–725. doi:10.1038/nrc3144
8. Moons KGM, de Groot JAH, Bouwmeester W, et al. Critical Appraisal and Data Extraction for Systematic Reviews of Prediction Modelling Studies: the CHARMS Checklist. *PLos Med*. 2014;11:12. doi:10.1371/journal.pmed.1001744
9. Tang DL, Kang R, Vanden Berghe T, Vandenabeele P, Kroemer G. The molecular machinery of regulated cell death. *Cell Res*. 2019;29:347–364. doi:10.1038/s41422-019-0164-5
10. Dixon SJ, Lemberg K, Lamprecht M, et al. Ferroptosis: an Iron-Dependent Form of Nonapoptotic Cell Death. *Cell*. 2012;149:1060–1072. doi:10.1016/j.cell.2012.03.042
11. Jiang XJ, Stockwell BR, Conrad M. Ferroptosis: mechanisms, biology and role in disease. *Nat Rev Mol Cell Biol*. 2021;22:266–282. doi:10.1038/s41580-020-00324-8
12. Yang WS, SriRamaratnam R, Welsch M, et al. Regulation of Ferroptotic Cancer Cell Death by GPX4. *Cell*. 2014;156:317–331. doi:10.1016/j.cell.2013.12.010
13. Ingold I, Berndt C, Schmitt S, et al. Selenium Utilization by GPX4 Is Required to Prevent Hydroperoxide-Induced Ferroptosis. *Cell*. 2018;172:409. doi:10.1016/j.cell.2017.11.048
14. Quail DF, Joyce JA. Microenvironmental regulation of tumor progression and metastasis. *Nat. Med*. 2013;19:1423–1437. doi:10.1038/nm.3394
15. Balkwill FR, Capasso M, Hagemann T. The tumor microenvironment at a glance. *J. Cell Sci*. 2012;125:5591–5596. doi:10.1242/jcs.116392
16. Binnewies M, Roberts EW, Kersten K, et al. Understanding the tumor immune microenvironment (TIME) for effective therapy. *Nat Med*. 2018;24:541–550. doi:10.1038/s41591-018-0014-x
17. Goodell V, Salazar LG, Urban N, et al. Antibody immunity to the p53 oncogenic protein is a prognostic indicator in ovarian cancer. *J Cli Oncol*. 2006;24:762–768. doi:10.1200/JCO.2005.03.2813

18. Zhang L, Conejo-Garcia JR, Katsaros D, et al. Intratumoral T cells, recurrence, and survival in epithelial ovarian cancer. *New Engl J Med*. 2003;348:203–213. doi:10.1056/NEJMoa020177
19. Schlienger K, Chu CS, Woo EY, et al. TRANCE- and CD40 ligand-matured dendritic cells reveal MHC class I-restricted T cells specific for autologous tumor in late-stage ovarian cancer patients. *Clin Can Res*. 2003;9:1517–1527.
20. Curiel TJ, Coukos G, Zou L, et al. Specific recruitment of regulatory T cells in ovarian carcinoma fosters immune privilege and predicts reduced survival. *Nat Med*. 2004;10:942–949. doi:10.1038/nm1093
21. Sato E, et al. Intraepithelial CD8(+) tumor-infiltrating lymphocytes and a high CD8(+)/regulatory T cell ratio are associated with favorable prognosis in ovarian cancer. *Proceedings Of The National Academy Of Sciences Of The United States Of America* **102**, 18538–18543, doi:10.1073/pnas.0509182102 (2005).
22. Broussard EK, Disis ML. TNM Staging in Colorectal Cancer: t Is for T Cell and M Is for Memory. *J Clin Onco*. 2011;29:601–603. doi:10.1200/jco.2010.32.9078
23. Zhou N, Bao J. FerrDb: a manually curated resource for regulators and markers of ferroptosis and ferroptosis-disease associations. *Database*. 2020;2020. doi:10.1093/database/baaa021
24. Stockwell BR, Jiang X, Gu W. Emerging Mechanisms and Disease Relevance of Ferroptosis. *Trends Cell Biol*. 2020;30:478–490. doi:10.1016/j.tcb.2020.02.009
25. Chen X, Kang R, Kroemer G, Tang D. Broadening horizons: the role of ferroptosis in cancer. *Nat Rev Clin Oncol*. 2021;18:280–296. doi:10.1038/s41571-020-00462-0
26. Costa I, Barbosa DJ, Benfeito S, et al. Molecular mechanisms of ferroptosis and their involvement in brain diseases. *Pharmacol Ther*. 2023;244:108373. doi:10.1016/j.pharmthera.2023.108373
27. Golia D'Auge T, CUCCU I, DE ANGELIS E, et al. Laparoscopic prediction of primary cytoreducibility of epithelial ovarian cancer. *Minerva Obstet Gynecol*. 2024. doi:10.23736/S2724-606X.24.05452-6
28. Perrone C, Angioli R, Luvero D, et al. Targeting BRAF pathway in low-grade serous ovarian cancer. *J Gynecol Oncol*. 2024;35:e104. doi:10.3802/jgo.2024.35.e104
29. Stockwell BR, Friedmann Angeli JP, Bayir H, et al. Ferroptosis: a Regulated Cell Death Nexus Linking Metabolism, Redox Biology, and Disease. *Cell*. 2017;171:273–285. doi:10.1016/j.cell.2017.09.021
30. Kapper C, Oppelt P, Arbeithuber B, et al. Targeting ferroptosis in ovarian cancer: novel strategies to overcome chemotherapy resistance. *Life Sci*. 2024;349:122720. doi:10.1016/j.lfs.2024.122720
31. Lee J, You JH, Shin D, Roh JL. Inhibition of Glutaredoxin 5 predisposes Cisplatin-resistant Head and Neck Cancer Cells to Ferroptosis. *Theranostics*. 2020;10:7775–7786. doi:10.7150/thno.46903
32. Zheng Z, Li Y, Jin G, et al. The biological role of arachidonic acid 12-lipoxygenase (ALOX12) in various human diseases. *Biomedi Pharmacot*. 2020;129:110354. doi:10.1016/j.biopha.2020.110354
33. Chu B, Kon N, Chen D, et al. ALOX12 is required for p53-mediated tumour suppression through a distinct ferroptosis pathway. *Nature Cell Biology*. 2019;21:579–591. doi:10.1038/s41556-019-0305-6
34. Zhang P, Gao K, Zhang L, et al. CRL2-KLHDC3 E3 ubiquitin ligase complex suppresses ferroptosis through promoting p14ARF degradation. *Cell Death Different*. 2022;29:758–771. doi:10.1038/s41418-021-00890-0
35. Koppula P, Zhuang L, Gan B. Cystine transporter SLC7A11/xCT in cancer: ferroptosis, nutrient dependency, and cancer therapy. *Protein Cell*. 2021;12:599–620. doi:10.1007/s13238-020-00789-5
36. Cicin-Sain L. Cytomegalovirus memory inflation and immune protection. *Medical Micro Immun*. 2019;208:339–347. doi:10.1007/s00430-019-00607-8
37. Klenerman P, Oxenius A. T cell responses to cytomegalovirus. *Nature Rev Immun*. 2016;16:367–377. doi:10.1038/nri.2016.38
38. O'Hara GA, Welten SPM, Klenerman P, Arens R. Memory T cell inflation: understanding cause and effect. *Trends in Immunology*. 2012;33:84–90. doi:10.1016/j.it.2011.11.005
39. Cicin-Sain L, Arens R. Exhaustion and Inflation at Antipodes of T Cell Responses to Chronic Virus Infection. *Trend Microb*. 2018;26:498–509. doi:10.1016/j.tim.2017.11.012
40. Shen Y, Zhu H, Shenk T Human cytomegalovirus IE1 and IE2 proteins are mutagenic and mediate "hit-and-run" oncogenic transformation in cooperation with the adenovirus E1A proteins. *Proceedings of the National Academy of Sciences* 1997;94:3341–3345. doi:10.1073/pnas.94.7.3341
41. Soroceanu L, Cobbs CS. Is HCMV a tumor promoter? *Virus Rese*. 2011;157:193–203. doi:10.1016/j.virusres.2010.10.026
42. Geisler J, Touma J, Rahbar A, Söderberg-Nauclér C, Vetvik K. A Review of the Potential Role of Human Cytomegalovirus (HCMV) Infections in Breast Cancer Carcinogenesis and Abnormal Immunity. *Cancers*. 2019;11:1842. doi:10.3390/cancers11121842
43. Herbein G. Tumors and Cytomegalovirus: an Intimate Interplay. *Viruses*. 2022;14(812). doi:10.3390/v14040812
44. Quentin L. Cytomegalovirus and Tumors: two Players for One Goal-Immune Escape. *Open Viro J*. 2011;5:60–69. doi:10.2174/1874357901105010060
45. Herbein G. High-Risk Oncogenic Human Cytomegalovirus. *Viruses*. 2022;14:2462. doi:10.3390/v14112462
46. Zhu L, Yang F, Wang L, et al. Identification the ferroptosis-related gene signature in patients with esophageal adenocarcinoma. *Cancer Cell Intern*. 2021;21:124. doi:10.1186/s12935-021-01821-2
47. Guo H, Bai R, Cui J. Advances in Combination Therapy of Immune Checkpoint Inhibitors for Lung Cancer. *Zhongguo Fei Ai Za Zhi*. 2020;23:101–110. doi:10.3779/j.issn.1009-3419.2020.02.05
48. Nguyen LT, Ohashi PS. Clinical blockade of PD1 and LAG3 — potential mechanisms of action. *Nature Revi Immu*. 2015;15:45–56. doi:10.1038/nri3790
49. Wang B. The Role of the Transcription Factor EGR1 in Cancer. *Front Oncol*. 2021;11. doi:10.3389/fonc.2021.642547
50. Boac BM, Xiong Y, Marchion DC, et al. Micro-RNAs associated with the evolution of ovarian cancer cisplatin resistance. *Gyneco Oncol*. 2016;140:259–263. doi:10.1016/j.ygyno.2015.12.026